

Comparison of semi- spherical solar collector with flat plate solar collector

Mojtaba Moravej ^{1*}, Fatemeh Namdarnia ², Leila Esmaili ²

¹ Department of mechanical engineering, Payame Noor University, Iran.

² Payame Noor University, Iran

*Corresponding author E-mail: moravej60@pnu.ac.ir

Abstract

The efficiency of each solar system depends on the amount of radiation that it receives. The evident characteristic of solar energy is its change throughout the day and during different seasons. Another feature of this energy is the change of position of the sun in the sky relative to Earth. The greatest amount of radiation from the sun comes when the sun's rays rise vertically to the desired level. For this reason, in solar collector systems, the collector must rotate to the sun, otherwise, the amount of accumulated energy falls. The purpose of this paper is to compare the performance of a solar semi- spherical collector with a flat plate collector. In this study, the semi- spherical solar collector does not need to be placed in a specific direction and also does not need the sunlight tracking mechanism to get the most amount of sunlight. Due to the semi- spherical shape of this collector, all geographic directions have the same effect. It also exhibits the highest resistance to wind blowing in terms of greater stability and lack of vibration and destruction. But the flat plate collector should be in the direction of radiation. In this research, experimental data from a flat plate collector in a closed cycle have been investigated with experimental data from a semi- spherical solar collector, simultaneously and it is shown that reducing the radiation or wind velocity will have the greatest impact on the flat plate collector and its outlet temperature. The experiments showed that the highest efficiency was in semi-spherical solar collector and it was about 67% and the highest outlet water temperature was in the flat collector and around 76°C.

Keywords: Solar Energy; Semi- Spherical Solar Collector; Flat Plate Solar Collector; Received Radiation; Efficiency.

1. Introduction

Collectors are divided into two fixed models and a moving tracker. The fixed collectors are divided into three categories, which heat transfer method will differ according to the division of them [1]. Selecting the collector type depends on the weather conditions of the area and the desired temperature (hot water temperature) and economic conditions. Although today, a variety of collectors are made with new and advanced technology, the adsorbent materials used have the maximum absorption and minimal emission and reflection [2].

Solar collector properties play an important role in efficiency value [3]. Scientists and engineers are seeking the new ways to increase the efficiency in order to increase the performance and decrease the expenses.

Tracking collectors even though produce high temperatures in all cases, because of their high cost their use is not cost-effective. For this reason, the use of constant collectors is more common. On the other hand, given the fact that throughout a year, the angle of the sun's irradiance and sun's altitude varies, the researchers in the industry have sought to further enhance this product [4].

Flat plate collectors are widely used in solar energy issues. Flat plate collectors and semi- spherical solar collectors are similar in terms of structure. These collectors are usually made up of a series of parallel tubes welded under a dark metal absorbent surface, and a glass or plastic covering above the adsorbent. The collector's around and below is also used insulator sheet to reduce the heat dissipation. Flat collectors are usually located in a steady position for

instance in the northern hemisphere is located to the south. [5] During a year, with changing the season and changing the orientation of the sun usually is turned toward the sun [6].

One of the most important features of these collectors is the ability to absorb and direct radiation simultaneously. One of the other benefits of this kind of collectors is no need for follow up the sun, navigation, and easy maintenance and repair. Because of its spherical shape, all of the geographic directions have the same effect, and because of its semi-spherical shape during day some of the surface is under direct radiation. In addition to its spherical shape, it exhibits the highest stability and disruption to the wind.

The experiments were carried out in winter at the Behbahan city in the south of Iran with geographic characteristics of 50 degrees and 14 minutes east longitude and 30 degrees and 36 minutes north latitude.

Nomenclature

T_i	Inlet fluid temperature of solar collector (K)
A_c	Surface area of solar collector (m ²)
T_o	Outlet fluid temperature of solar collector (K)
C_p	Heat capacity(J/Kg k)
$T_{o,i}$	Collector outlet initial coolant temperature (K)
D_T	Difference between inlet-outlet temperatures (0 C)
$T_{o,t}$	Collector outlet coolant temperature after time t (K)
F_R	Heat removal factor
U_l	Overall loss coefficient of solar collector (W/m ² K)
G_T	Global solar radiation (W/m ²)
\dot{m}	Mass flow rate (Kg/s)
α_τ	Absorption-transmittance product
Q_u	Rate of useful energy gained (W)
η_i	Instantaneous collector efficiency

S_η Uncertainty of efficiency (%)
τ Time constant of conical collector
T_a Ambient temperature (K)

2. Materials and methods

2.1. Governing equations

The useful energy gained by the fluid passing through the collector is [7]:

$$Q_u = \dot{m}C_p (T_{out} - T_{in}) \tag{1}$$

In the above relation, T_{in} and T_{out} respectively, the temperature of the inlet and outlet of the fluid from the collector and, C_p and \dot{m} respectively, the specific heat and mass flow rate of the fluid. [7] The useful energy obtained by the collector in terms of the amount of solar radiation input and the heat loss of the collector body is bellow [7].

$$Q_u = A_p F_R [S - U_l (T_m - T_a)] \tag{2}$$

In the above relation T_a is the ambient temperature and F_R is the heat removal coefficient, which is defined as follows [7].

$$F_R = \frac{\dot{m}C_p}{U_l A_p} [1 - \exp(-FU_l A_p / \dot{m}C_p)] \tag{3}$$

S is part of the solar radiation absorbed by the collector absorber surface area. S is obtained from the following equation [7].

$$s = (\tau\alpha)I_T = \eta_o I_T \tag{4}$$

That the I_T solar flux entered into the collector and η_o is the optical efficiency and is an effective product of cross-absorption which is obtained from following relationship [7].

$$\eta_o = (\tau\alpha) = 1.01\tau\alpha \tag{5}$$

In steady state, the useful energy received by the collector is:

$$Q_u = A_p S - U_l A_p (T_p - T_a) \tag{6}$$

T_p is the absorber plate temperature and U_l is the overall drop from the collector [7].

2.2. Specifications of the system and description of the tests

The properties and real photo of experiment and instruments are shown in figure 1, Table 1 and 2.



Fig. 1: A View of the Flat Plate and Semi-Spherical Solar Collectors.

Table 1: The Characteristics of Semispherical Solar Collector

Characteristics	Dimension	Unit
<ul style="list-style-type: none"> Glass radius 		
A transparent glass sheet with a thickness of 6 mm install as a cover on the metal which allows the passage of light but it reduces the loss of heat transfer by stacking the air between the absorber and the glass and reduces heat dissipation.	43	cm
Coverage	12.1 22.0 67.	w/m.c ²
<ul style="list-style-type: none"> Conducting Density Specific Heat Reflection coefficient Absorption coefficient Dispersion coefficient Absorbent radius 	.794. .386. 526.1	g/cm ³ J/kg.c ²
Absorber	39	cm
A high temperature thermal conductive absorber made of iron and its surface is darkened by the use of a bluish black color which absorbs solar energy better. The thickness of the sheet metal is 3 millimeters.	4.8 10.25	w/m.c ²
<ul style="list-style-type: none"> Conducting Specific Heat Density Type of absorber coating Absorption coefficient 	87.37 Opaque black color 9.	J/kg.c ² g/cm ³
Tubes	3.8	
Copper tubes soldered to the absorber surface and the fluid inside the tubes receives heat from the absorber. The diameter of these pipes is 3.8 inches.		
Working fluid		J/kg.c ² g/cm ³
<ul style="list-style-type: none"> A heat transfer fluid which is water in this experiment that absorbs heat from the absorber surface. Specific heat capacity Density A heat insulator placed under the collector and has a thickness of 2 centimeters. It is usually made of polystyrene which reduces heat dissipation. Insulating glass wool 2 centimeters thick, wrapped around the metal beneath the collector to prevent 		
Insulation		

<ul style="list-style-type: none"> heat loss by the collector's below metal surface. Insulation tank A domestic water purifier pump for pumping water inside the reservoir into the collector.

Table 2: The Characteristics of Flat Plate Solar Collector

Characteristics	Dimension	Unit
<ul style="list-style-type: none"> Glass 		
A transparent glass sheet with a thickness of 6 mm install as a cover on the metal which allows the passage of light but it reduces the loss of heat transfer by stacking the air between the absorber and the glass and reduces heat dissipation.	100	cm
Coverage	12.1 22.0 77.0	w/m.c ²
<ul style="list-style-type: none"> Conducting Density Specific Heat Reflection coefficient Absorption coefficient Dispersion coefficient Absorbent 	0.794 2386 526.1	g/cm ³ J/kg.c ²
A high temperature thermal conductive absorber made of iron and its surface is darkened by the use of a bluish black color which absorbs solar energy better. The thickness of the sheet metal is 3 millimeters.	90	cm
Absorber	4.8 1.25 87.37 Opaque black color 9.0	w/m.c ² J/kg.c ² g/cm ³
<ul style="list-style-type: none"> Conducting Specific Heat Density Type of absorbent coating Absorption coefficient 		
Tubes	Copper tubes soldered to the absorber surface and the fluid inside the tubes receives heat from the absorber. The diameter of these pipes is 3.8 inches.	3.8
Working fluid	<ul style="list-style-type: none"> A heat transfer fluid which is water in this experiment that absorbs heat from the absorbent surface. Specific heat capacity Density A heat insulator placed under the collector and has a thickness of 2 centimeters. It is usually made of polystyrene which reduces heat dissipation. 	J/kg.c ² g/cm ³
Insulation	<ul style="list-style-type: none"> Insulating glass wool 2 centimeters thick, wrapped around the metal beneath the collector to prevent heat loss by the collector's below metal surface. Insulation tank A domestic water purifier pump for pumping water inside the reservoir into the collector. 	

The experiments were carried out in winter at the behbahan city in the south of Iran with geographic characteristics of 50 degrees and 14 minutes east longitude and 30 degrees and 36 minutes north latitude.

The characteristics of both solar collector used in this experimental test are given in Table 1 and 2.

The solar semispherical collector used in this work is made by the authors in Payame noor University of Iran.

Experiments were performed with different flow rates of 0.005, 0.108, 0.0133, 0.126, 0.166 kg/s. Each flow rate has been tested several times and the data of the tables is the average of the data. The wind speed was measured from 0.2 to 8.2 m/s on the test days. During the experiment, ambient temperature, temperature of collector absorber surface and collector glass surface and inlet and outlet water were measured by thermocouples (type K) that these sensors were connected to a channel data logger (TES data logger model). The solar radiation was recorded by a solar meter, also these measures are recorded every half an hour.

3. Testing method

ASHRAE Standard 86-93 for testing the thermal performance of collector is certainly the most often used to evaluate the performance of stationary solar collectors [8] (shown in table 2). The thermal performance of the solar collector is determined by obtaining the values of instantaneous efficiency for different combination of incident radiation, ambient temperature and inlet fluid temperature [9, 10].

According to ASHRAE Standard 86-93, steady-state conditions should be prepared during the data period and also during a specific time interval prior to the data period, this is called pre-data period. To reach steady-state variables must be in a specific limitation as defined in Table 3 in the entire test period.

The standard according to which these experiments were carried out is the ASHRAE 93 standard which the general conditions are listed in the table below [11].

Table 3: Standard Test Conditions (ASHRAE 93)

Parameter	unit	ASHRAE 93
Accuracy of temperature cold water inlet	°C	± 1
Accuracy of temperature difference across hot water system	°K	± 0.5 (°C)
Precision of temperature difference across hot water system	°K	± 0.2 (°C)
Ambient air temperature position	---	At a distance of 1.2 m above the ground and at a minimum distance of 1.5 m from the reservoir and the system
Pipe Lengh	M	15
Pyranometer	---	Class I
Accuracy of temperature ambient air	°C	± 0.5
Precision of temperature ambient air	°C	± 0.2
Accuracy of the liquid flowrate measurement	% mass per unit time	± 1
Mass measurement	%	± 1

3.1. Description of device calibration

Calibration of measuring instruments were undertaken before, during and after the experimental data collection. Thermocouples were calibrated by using an independently calibrated platinum resistance thermometer; flow meter used a data-logging sub-routine to draw water from the systems into a container and measuring the mass with accuracy scales, and solar meter used a calibrated reference solar meter with a valid calibration certificate. The accuracy of thermometer data logger is 0.1 and accuracy of flow meter is 0.05 kg/min. tracking of total solar radiation was implemented by a TES 132 solar meter type with an accuracy of 1 w/m².

3.2. Error analysis

Due to ASME guidelines, there are not absolute measurements and errors in any experimental measurement. Some of the usual sources of error are: the errors of calibration, data recording errors and inappropriate instruments [12], [13]. Errors in flow rate measurement,

temperature measurement and solar radiation measurement are the main components to uncertainty in collector efficiency. The uncertainty results of the measurements including all the sources of errors are shown in Table 4.

In measuring any quantity, we usually each measurement several times repeated in exactly the same conditions with a definite device. This action reduces some of the error factors. The average value of the measured values is the best and most likely value of the quantity.

Table 4: Results of Uncertainty in the Present Work

Parameter	Uncertainty (%)
Volumetric flow rate	±0.5
Solar radiation	±5
Difference between inlet-outlet temperature	±1.1

The combined uncertainty for calculation the collector efficiency, $S\eta$, was determined by the root sum square method (RSS), based on Eq. (8) [14].

This analysis as Eq. (9). We assume that errors in C_p and A_c are negligible.

$$\int S\eta = \sqrt{\left(\frac{\Delta m}{m}\right)^2 + \left(\frac{\Delta G}{G}\right)^2 + \left(\frac{\Delta(\Delta T)}{\Delta T}\right)^2} \tag{9}$$

Where $\Delta m/m$ is flow rate changes and $\Delta G/G$ received radiation changes and $\Delta(\Delta T)/\Delta T$ are used to measure the variation in the temperature of the inlet and outlet of the working fluid.

The maximum uncertainty determined in the present work in calculation the collector efficiency, at several tests was about 6%.

4. Results and discussion

In the later sections and in sequence, using the results of the experiments, first, the working fluid used in the test will be investigated and then the temperature of the inlet and outlet water and the difference in temperature of the outlet and input water in term of time and in term of received radiation will be analyzed and in the end the efficiency and the factors affecting it will be reviewed.

All data are tested in a quasi-steady state condition. The collector is perpendicular to the ground and used water as working fluid. The tests of the collector took place during several days in winter 2017 which were carried out during the day from 8:00 to 16:00 o'clock. The data were logged every 15 minutes. Figure 6 presents the solar radiation and temperatures profile in one the test days. In this figure, sun radiation and key temperature of a selective day versus local time are shown. It is clear that the maximum received radiation is near the solar noon.

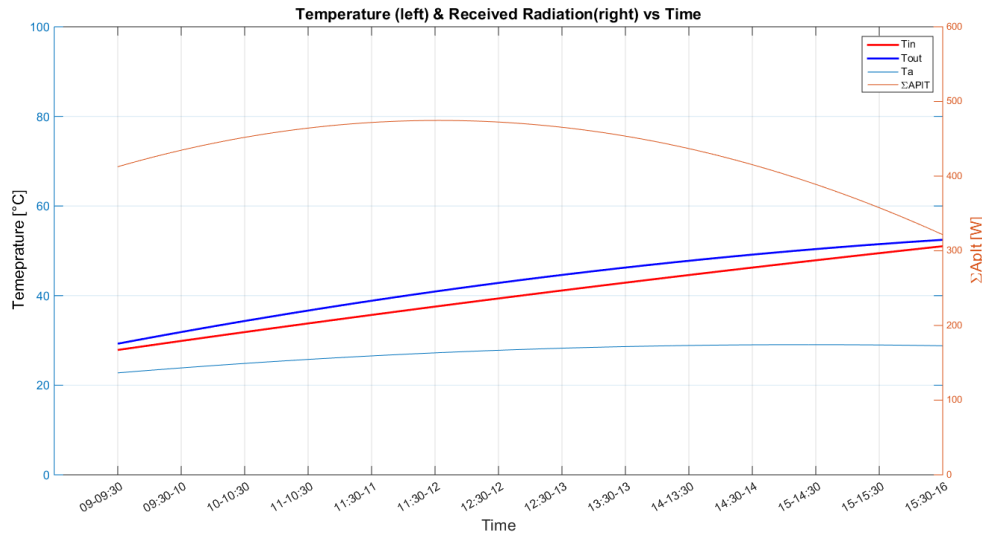


Fig. 2: Input and Output Water Temperature Changes, Received Radiation and Ambient Temperature for A Semi- Spherical Solar Collector in A Mass Flow Rate of (M) = 0.020kg.S-1.

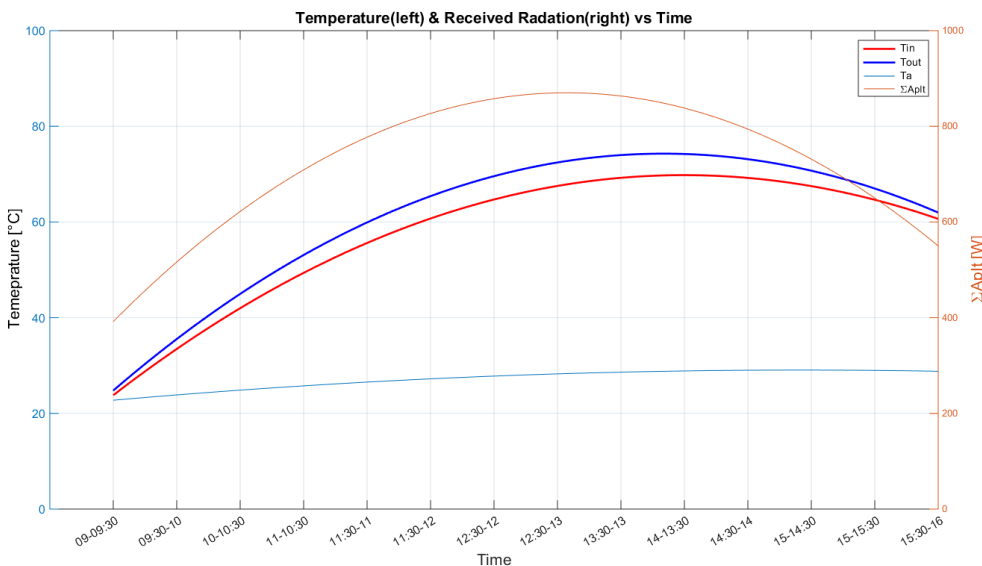


Fig. 3: Input and Output Water Temperature Changes, Received Radiation and Ambient Temperature for Flat Collectors with Mass Flow Rate (M = 0.022 Kg.S-1).

For a comparison of the performance of solar collector and the semi-spherical collector with each other under the same conditions, we consider a flat collector with an area of 1 square meter, which is equal to the semi-spherical solar collector's lateral area. The slope of flat plate collector is 35 degrees.

In diagram, radiation rates are lower in the early hours of the day and as the noon approaches, it increases and decreases around the evening, except during cloudy days, the radiation rate may be reduced around noon due to cloudiness of the air. In all days, because the test system is a closed system as a result the inlet water temperature has increased gradually. In all days, the outlet temperature has increased with time and approaching noon and even if the radiation rate is reduced as a result of reduction of direct sunlight, the graph of the temperature of the outlet water is increasing which indicates this collector using a 6 mm glass cover keeps the absorbed heat well, also indicates the capability of this type of collector in absorbing indirect radiation, which includes reflection and passive radiation [15].

In all situations for both collectors, input radiation rate between morning and midnight increases and then decreases. Energy efficiency also shows a similar tendency. However, the reason for lowering energy efficiency in the afternoon is the increase in the temperature of the inlet fluid, as well as the increase in the temperature of the adsorbent plate over time, which exacerbates the slippage.

As the inlet temperature increases, the output fluid temperature also increases which increases the efficiency. On the other hand, increasing the temperature of the inlet water means increasing the

temperature of the fluid inside the collector which increases the thermal drop, therefore, there is an optimal inlet water temperature which, for more temperatures, will reduce the efficiency we are seeing too much heat loss.

As shown in figure 2, with passing time and approaching noon, the ambient air temperature, the inlet and outlet water temperature and the intensity of the radiation are increased, over time and reduction of radiation rates we see the decrease in the outlet and inlet water temperature noticeably. If, as shown in figure 1, in the semi-spherical solar collector, even with decreasing radiation rates in the afternoon there is an increase in the temperature of the outlet water for hours.

Hourly efficiency of both types of collector is compared in figures 4 and 5. It is seen in the diagrams that during some hours the efficiency of the flat plate collector is higher and in some hours the efficiency of the semi-spherical is higher. In all tests has been observed the half-spherical collector efficiency in the early hours of the day that radiation is not direct is more than a flat plate collectors efficiency, this indicates another hypothesis regarding the shape of the semi-spherical collector in receiving the highest amount of radiation. However, in the afternoon is observed a decrease in hourly efficiency for a flat plate collector but it is seen that efficiency in the semiconductor collector still tends to increase this also reflects the proper structure of this collector to maintain heat within itself.

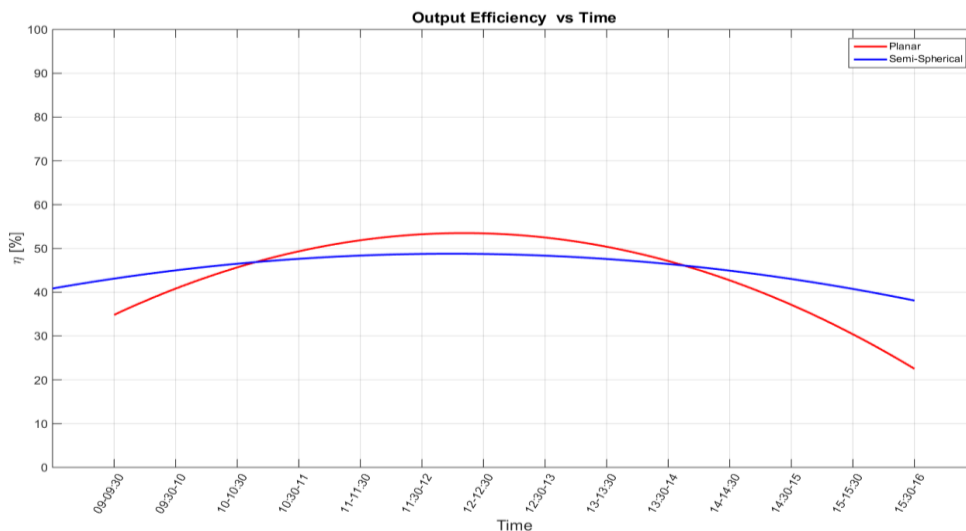


Fig. 4: Check the Efficiency of the Two Collectors Every Half Hour.

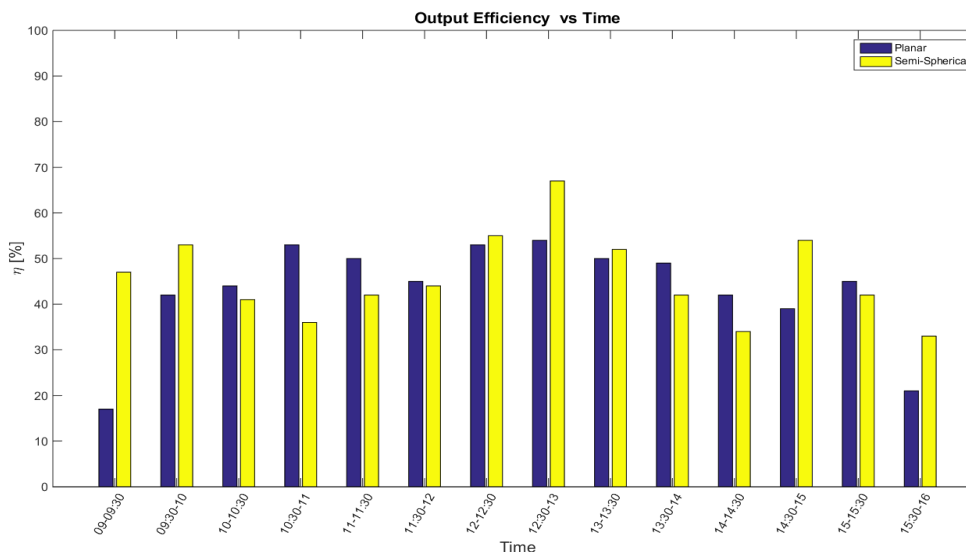


Fig. 5: Comparison of the Efficiency of Two Collectors.



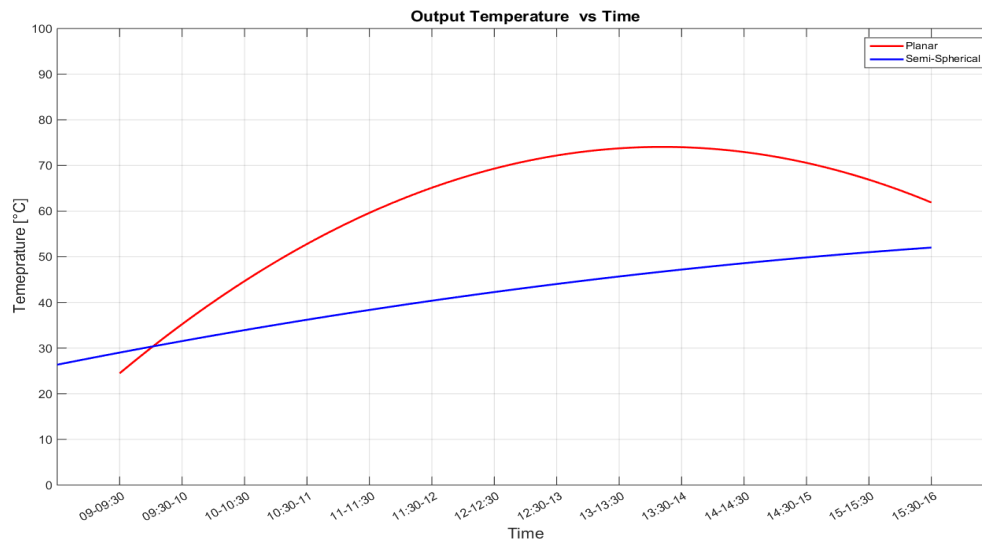


Fig. 6: The Graph of the Temperature of the Output of Both Collectors per Half Hour.

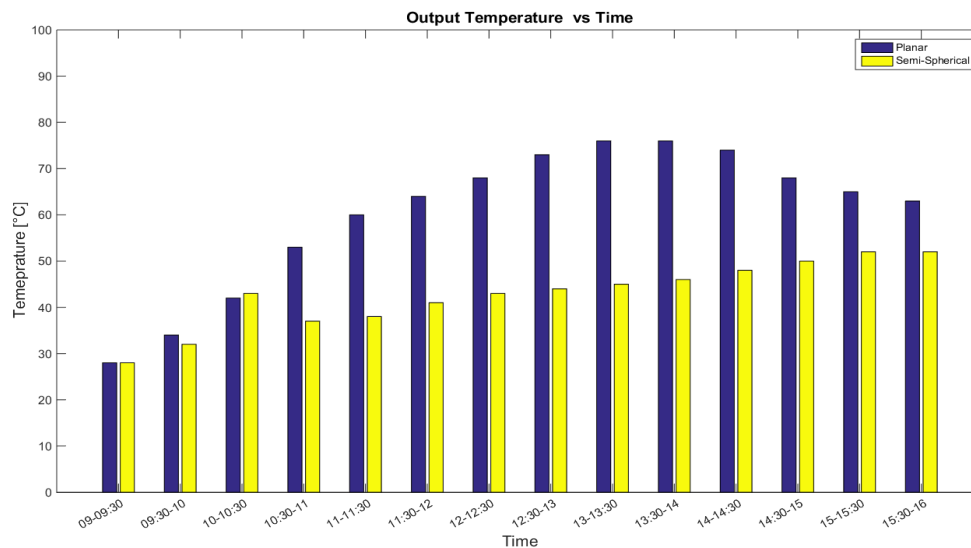


Fig. 7: Comparison of the Output Temperature of Both Collectors.

Maximum efficiency for flat collector is 54% and for a semi-spherical collector is 67%. Of course, the highest warm water temperature has been achieved, it was taken by a flat plate collector that reached over 76 degrees Celsius but for the semi-spherical collector, the maximum water temperature reached 52 °C.

- Flat collectors under direct sunlight (in the mid-hours of the day when radiation is intense and direct) In the shortest possible time reached the water to temperatures above 70 °C If the radiation is constant and the wind is not tangible, stay at this temperature, otherwise the semi-spherical solar collector was not able to deliver water at such a temperature during testing days. But it was observed that with the wind blowing temperature of the output immediately began to decrease so that it will drop to about ten degrees of water temperature. But according to the winds or changes in the radiation rate, there is no immediate and significant impact on the water temperature of the collector's semi-spherical. This represents the structural stability of this type of collector against wind blowing and maintaining heat within itself.
- In experiments, the maximum difference between the input and output water temperature was about 7 to 8 degrees in the flat plate collector and in the semi-spherical solar collector, this amount reached at 5.5 degrees and both belong to the period from 11:30 to 13:30, of course, the numbers presented in the tables of test days are average number and numbers are entered in the mean.

- In the early and late hours of the day, the efficiency of the semi spherical collector was more than flat plate which, as already said, because at these times, sun radiation is not direct and the structure of this collector is designed in such a way which, given its semi-spherical shape, is capable of receiving the highest amount of radiation from all its directions. Conclusion:
- The outlet water temperature from the flat plate collector at all hours except the early hours of the morning was higher than the outlet temperature of the semi-spherical solar collector.
- From the study of efficiency during the test period, it can be seen that in the first and the last hours of the day when radiation is decrease, the semi-spherical collector's efficiency (due to the higher amount of radiation due to its semi-spherical shape) is higher but in the middle of the day, according to the graphs and corresponding shapes, the efficiency of the flat plate collector is higher.
- The effect of reducing the radiation rate on the outlet water temperature in the flat plate collector is very tangible and abruptly reduced the temperature of the outlet water, this is not the case with semi-spherical solar collector.
- The effect of wind blowing on the outlet water temperature in the flat plate collector is very tangible and sometimes observed up to ten degrees reduction this is not the case with semi-spherical solar collector.

- The highest efficiency was in semi-spherical solar collector and it was about 67% and the highest outlet water temperature was in the flat collector and around 76°C.

References

- [1] S. Riffat, X. Zhao P. S. Doherry: Developing a theoretical model to investigate thermal performance of a thin membrane heat-pipe solar collector, *Applied Thermal Engineering* 25(2005) 899-91. <https://doi.org/10.1016/j.applthermaleng.2004.08.010>.
- [2] F. Cruz-Peragon, J.M. Palomar, P.J. Casanova, M.P. Dorado, F. Manzano-Agugliaro, Characterization of solar flat plate collectors, *Journal of Science Direct*, 16, April 2012, Pages 1709–1720 <https://doi.org/10.1016/j.rser.2011.11.025>.
- [3] M. Abdolzadeh, M. A. Mehrabian: The optimal slope angle for solar collectors in hot and dry parts of Iran, *Energy Sources* 34 (2012) 519-530. <https://doi.org/10.1080/15567036.2011.576413>.
- [4] S. Kalogirou, “Solar thermal collectors and applications”, *Progress in energy and combustion science*, 30 (2004) 231-295. <https://doi.org/10.1016/j.pecs.2004.02.001>.
- [5] Y. Tian, C. Y. Zhao, “A review of solar collectors and thermal energy storage in solar thermal applications”, *Applied Energy*, 104 (2013) 538-553. <https://doi.org/10.1016/j.apenergy.2012.11.051>.
- [6] LM. Ayompe, A. Duffy: Analysis of the thermal performance of a solar water heating system with flat plate collectors in a temperate climate, *Applied Thermal Engineering* 58 (2013) 447-454. <https://doi.org/10.1016/j.applthermaleng.2013.04.062>.
- [7] Z. Sen, *Solar Energy Fundamentals and Modeling Techniques*, Springer, 2008.
- [8] ASHRAE Standard 93-86, *Methods of testing and determine the thermal performance of solar collectors*, ASHRAE: Atlanta (2003).
- [9] J.A. Duffie, W.A. Beckman, “*Solar Engineering of Thermal Processes*”, fourth ed., Wiley, New York, 2013. <https://doi.org/10.1002/9781118671603>.
- [10] D. Rojas, J. Beermann, S.A. Klein, D.T. Reindl, “Thermal performance testing of flat plate collectors”, *Solar Energy*, 82 (2008) 746-757. <https://doi.org/10.1016/j.solener.2008.02.001>.
- [11] K. Guthrie, M. Maffucc, International standards for solar water Heaters, *Journal of Science Direct*, 2012, 30: Pages 1304–1310. <https://doi.org/10.1016/j.egypro.2012.11.143>.
- [12] R. B. Abernethy, R. P. Benedict, R. B. Dowdell, “ASME measurement uncertainty”, ASME paper, 1983, 83-WA/FM-3.
- [13] J. Ma, W. Sun, J. Ji, Y. Zhang, A. Zhang, W. Fan, “Experimental and theoretical study of the efficiency of a dual-function solar collector”, *Applied Thermal Engineering*, 31 (2011) 1751-1756. <https://doi.org/10.1016/j.applthermaleng.2011.02.019>.
- [14] Tongtuama. Y, Ketjoya. N, Vaivudha. S and Thanaraka. P, Effect of the diffuse radiation reflection from exterior wall on Shading Device Integrated Photovoltaic case of Thailand building, *Journal of Science Direct*, No. 9, 2011, pp. 104 –116. <https://doi.org/10.1016/j.egypro.2011.09.012>.
- [15] J. Boland, J. Huang, B. Ridley, Decomposing global solar radiation into its direct and diffuse components, *Journal of Science Direct*, No. 28, 2013, pp. 749 – 756. <https://doi.org/10.1016/j.rser.2013.08.023>.